

CHAPTER IV

RESULTS

The body mass index (BMI) of pregnancies and fetal birth weight

The pregnant women who live in non-Cd and Cd contaminated areas were a total of 51 cases, participating in this study. Among of them, 28 cases were from non-Cd contaminated area and another 23 cases were from Cd contaminated area. The maternal ages were in range of 18-39 years old. The results of maternal weight (68.78 ± 3.86 kg) and height (1.55 ± 0.01 m) of Cd contaminated group were similar with the maternal weight (65.26 ± 2.09 kg) and height (1.58 ± 0.01 m) of non-Cd contaminated group. However, the fetal birth weight of both non-Cd (3.09 ± 0.12 kg) and Cd contaminated groups (3.15 ± 0.1 kg) were not different. All data were shown in Table 7.

Table 7 The maternal weight, height and fetal birth weight of non-Cd and Cd contaminated groups

Group	Maternal weight (kg)	Maternal height (m)	Fetal birth weight (kg)
non-Cd contaminated group	65.26 ± 2.09 (n=23)	1.58 ± 0.01 (n=23)	3.09 ± 0.12 (n=10)
Cd contaminated group	68.78 ± 3.86 (n=15)	1.55 ± 0.01 (n=15)	3.15 ± 0.1 (n=10)

Values represent as mean \pm SEM.

The concentration of serum ferritin, placental Fe, blood Cd, urinary Cd and placental Cd.

The full term placentas were collected from pregnancies living in Cd and non-Cd contaminated areas, Mae Sot, Tak, Thailand. The mean of serum ferritin (19.26 ± 1.35 ng / mL) and placental iron accumulation (57.68 ± 4.72 mg/kg) of non-Cd contaminated group were similar to that the mean of serum ferritin and placental iron concentration of Cd contaminated group which were 23.00 ± 3.51 ng/mL and 57.11 ± 6.12 mg/kg, respectively. The Cd concentration in maternal blood (1.30 ± 0.21 ug/L) and placenta (20.31 ± 4.68 ug/kg) of Cd contaminated group were significantly higher than Cd concentration in maternal blood (0.67 ± 0.1 ug/L) and placenta (9.14 ± 0.72 ug/kg) of non-Cd contaminated group ($*p < 0.05$). Finally, the urinary Cd was also measured. The result also showed that the Cd concentration in urine (2.20 ± 0.41 ug/g creatinine) of Cd contaminated group trend to be higher than that of non-Cd contaminated group (1.51 ± 0.18 ug/g creatinine). All data were shown in Table 8.

Table 8 The concentration of serum ferritin, placental Fe, blood Cd, urinary Cd and placental Cd of non-Cd and Cd contaminated groups

Group	Blood Cd (ug/L)	Urinary Cd (ug/g creatinine)	Placental Cd (ug/kg)	Serum ferritin (ng/mL)	Placental Fe (mg/kg)
non-Cd contaminated group	0.67 ± 0.1 (n=25)	1.51 ± 0.18 (n=24)	9.14 ± 0.72 (n=24)	19.26 ± 1.35 (n=28)	57.68 ± 4.72 (n=24)
Cd contaminated group	$1.30 \pm 0.21^*$ (n=21)	2.20 ± 0.41^a (n=21)	$20.31 \pm 4.68^*$ (n=17)	23.00 ± 3.51 (n=23)	57.11 ± 6.12 (n=18)

Values represent as mean \pm SEM. ($*p < 0.05$)

^a $p=0.06$

According to Table 8, we analyzed the association between Cd concentration in maternal blood and placenta as shown in figure 29. The maternal blood Cd showed a significantly positive correlation with placental Cd concentration. The Pearson's strength of correlation coefficient value (r) was 0.699 ($*p = 0.0001$), the regressive coefficient value (r^2) was 0.489.

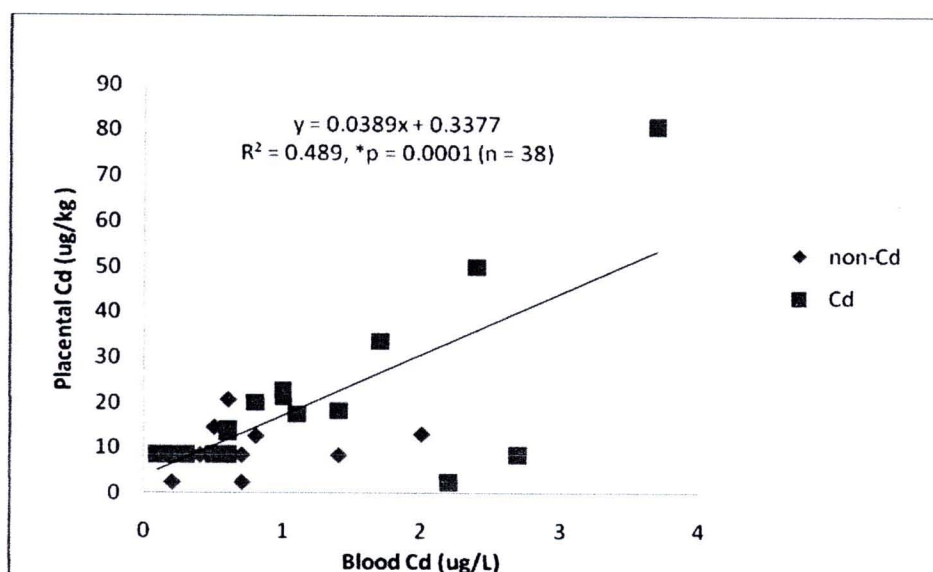


Figure 29 The correlation between Cd concentration in maternal blood and placental tissue (n=38, *p = 0.0001)

The relationship between blood Cd concentration and urinary Cd was also analyzed and showed in figure 30. The maternal blood Cd showed a significantly positive correlation with the urinary Cd concentration ($n = 38$). The Pearson's strength of correlation coefficient value (r) was 0.688 ($*p = 0.0001$), the regressive coefficient value (r^2) was 0.474.

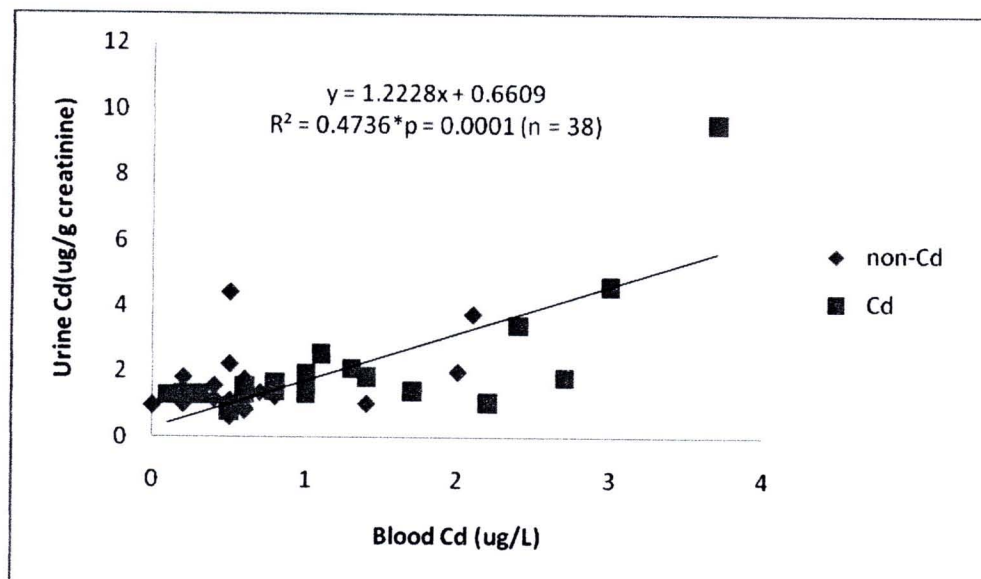


Figure 30 The correlation between Cd concentration in maternal blood and urine (n=38, *p = 0.0001)

The relationship between placental Cd and placental Fe concentration of all participants in non-Cd and Cd contaminated groups were shown in figure 31. The placental Cd trended to be an inverse correlation with the placental Fe even though this correlation was not significantly statistical analysis. The Pearson's strength of correlation coefficient value (r) was -0.117 ($p = 0.464$), the regressive coefficient value (r^2) was 0.0138 .

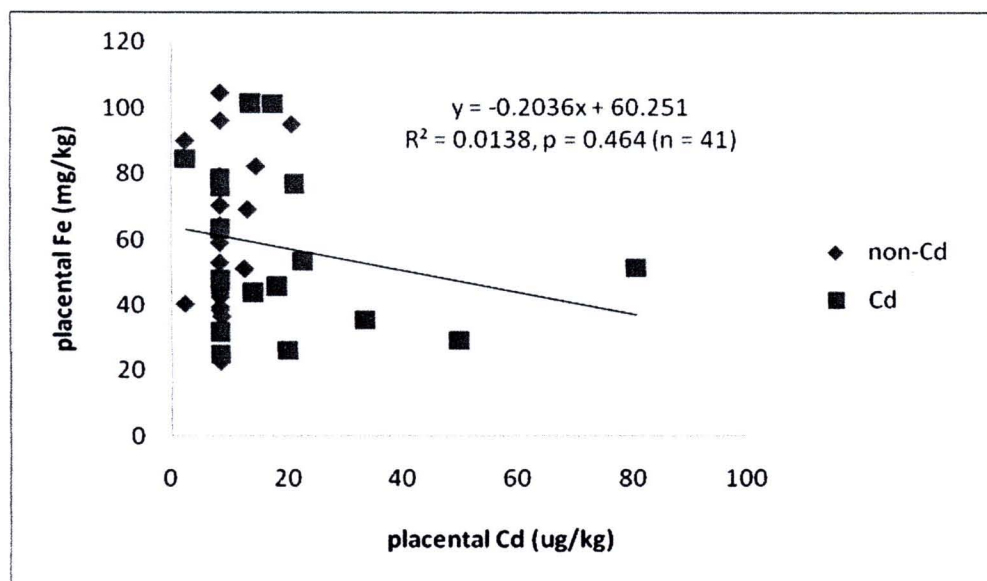


Figure 31 The correlation between placental Cd and placental Fe (n=41)

Among all of samples obtained from pregnancies living in Cd contaminated area, six of them were used and classified as high-Cd group. Also, 6 samples obtained from pregnancies living in non-Cd contaminated area were selected and classified as low-Cd group. The mean of Cd concentration in maternal blood ($1.83 \pm 0.43 \mu\text{g/L}$), placenta ($37.55 \pm 9.90 \mu\text{g/kg}$) of high- Cd group were significantly higher than that in low-Cd group which were $0.40 \pm 0.06 \mu\text{g/L}$ and $7.50 \pm 1.00 \mu\text{g/kg}$, respectively. Whereas, the mean of Cd concentration in urine ($3.16 \pm 1.31 \mu\text{g/g creatinine}$) of high-Cd group was not significantly difference compared to that of low-Cd group ($1.16 \pm 0.10 \mu\text{g/g creatinine}$). The serum ferritin of high-Cd ($28.65 \pm 9.26 \text{ ng/mL}$) and low-Cd groups ($20.43 \pm 3.71 \text{ ng/mL}$) were similar. Also, the placenta iron accumulated values of high-Cd ($40.20 \pm 4.72 \text{ mg/kg}$) and low-Cd groups ($43.86 \pm 3.11 \text{ mg/kg}$) were not significantly different. All data were shown in Table 9.

Table 9 The concentration of blood Cd, placental Cd, urinary Cd, serum ferritin and placental Fe of low-Cd and high-Cd groups

Group	Blood Cd ($\mu\text{g/L}$)	Placental Cd ($\mu\text{g/kg}$)	Urinary Cd ($\mu\text{g/g creatinine}$)	Serum ferritin (ng/mL)	Placental Fe (mg/kg)
low-Cd group	0.40 ± 0.06 (n=6)	7.50 ± 1.00 (n=6)	1.16 ± 0.10 (n=6)	20.43 ± 3.71 (n=6)	43.86 ± 3.11 (n=6)
high-Cd group	$1.83 \pm 0.43^*$ (n=6)	$37.55 \pm 9.90^*$ (n=6)	3.16 ± 1.31 (n=6)	28.65 ± 9.26 (n=6)	40.20 ± 4.72 (n=6)

Values represent as mean \pm SEM. (* $p < 0.05$)



Localization of DMT-1 protein in placental tissues

1. Fetal portion of placental tissues

In the term human placental tissues, the immunohistochemistry of DMT-1 in the placental tissues were observed under LM (Nikon Eclipse 80i). We found the immunoreactivity of DMT-1 localized in syncytiotrophoblastic layer (Figure 32A). High magnification (100X) was performed in order to see more details of DMT-1 protein expression. DMT-1 immunoreactivity showed a markedly diffuse in syncytiotrophoblastic cell (STB), especially in apical portion of cytoplasm and also presented at basal portion of syncytiotrophoblastic cell (Figure 32B). It was also shown uncounterstain slide (Figure 32C). The result showed that DMT-1 was localized in cytoplasm of STB. The negative control slide which omitted the primary antibody was and observed at 100X magnification as shown in Figure 32D. The DMT-1 positive tissue control, rat kidney tissue was done and observed at 40X magnification as shown in Figure 32E. Finally, the negative control of kidney tissue was shown in Figure 32F.

In addition, DMT-1 was localized in fetal capillary (Figure 33A). High magnification (100X) was performed in order to see more details. DMT-1 was likely intense only in cytoplasm of the endothelial cells (Figure 33B). It was also shown in uncounterstain slide (Figure 32C). The result showed that DMT-1 was localized in cytoplasm of fetal capillary. The negative control slide which omitted the primary antibody was and observed at 100X magnification as shown in Figure 33D. The DMT-1 positive tissue control, rat kidney tissue was done and observed at 40X magnification as shown in Figure 32E. Finally, the negative control of kidney tissue was shown in Figure 33F.

Moreover, DMT-1 was also localized in macrophage cell or so called hofbuaer cell observed at 40X and 100X magnifications as shown in Figure 34A and 34B.

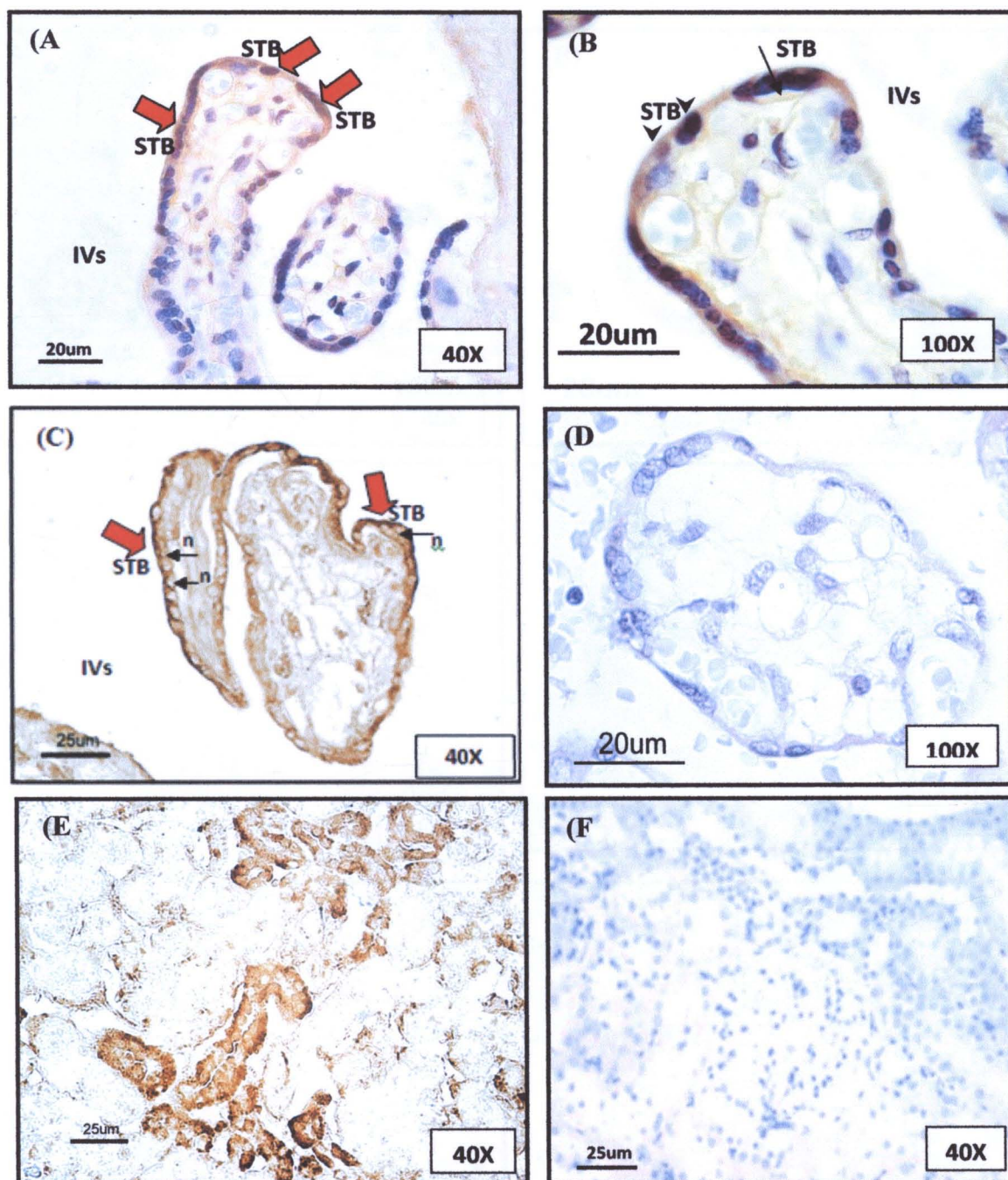


Figure 32 Localization of DMT-1 in STB (A; red arrow), (B) DMT-1 was localized in apical surface of cytoplasm (arrow head) and basal surface (black arrow) of STB, (C) DMT-1 was localized in only cytoplasm (red arrow) of STB, (D) negative control of placenta, (E) DMT-1 positive tissue control (kidney), (F) negative control of kidney. STB; Syncytiotrophoblast cells, n; nucleus, IVs; Intervillous space

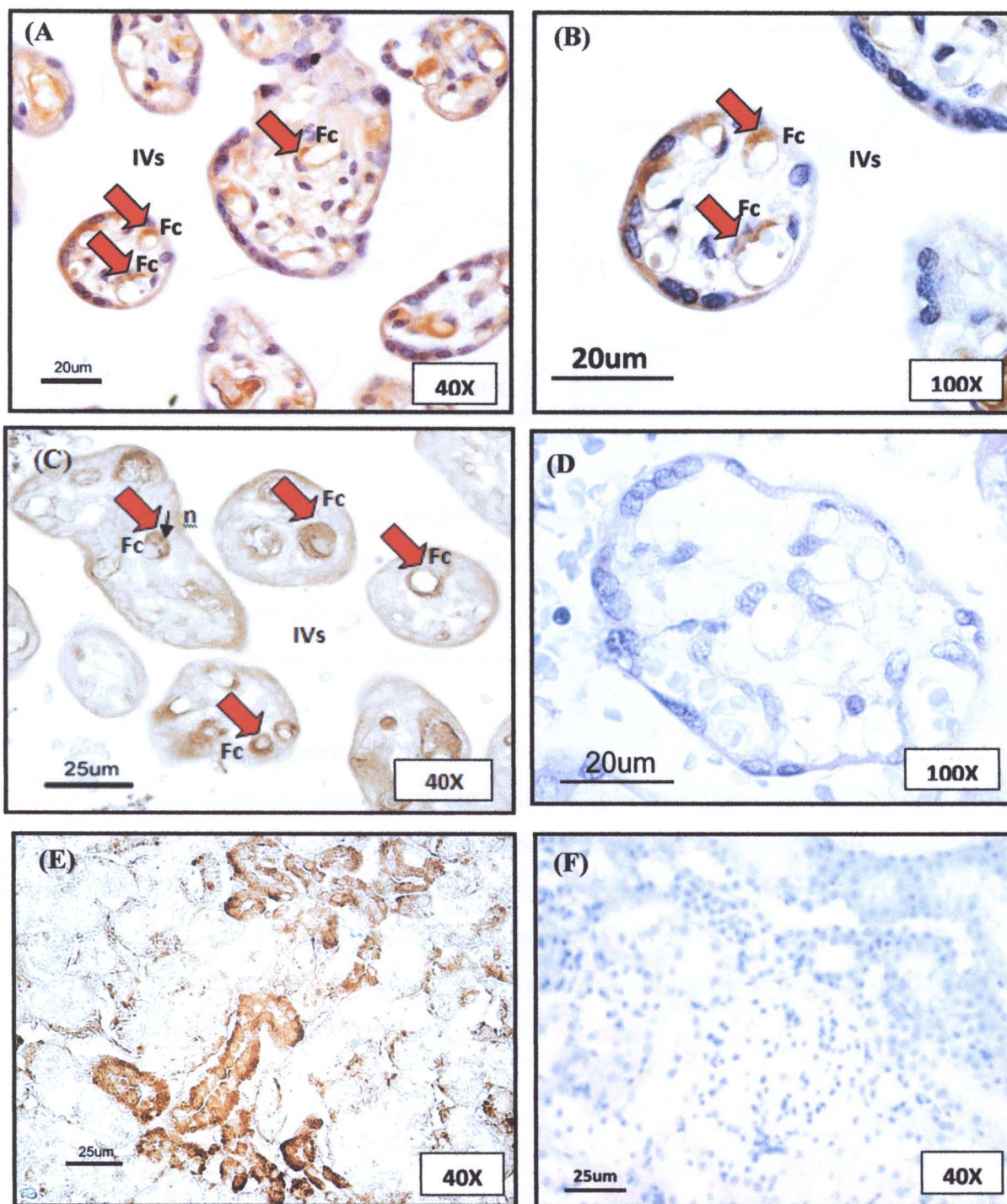


Figure 33 Localization of DMT-1 in fetal capillary (A; red arrow), DMT-1 was localized only in cytoplasm of endothelial cells of fetal capillary (B, C; red arrow), (D) negative control of placenta, (E) DMT-1 positive tissue control (kidney), (F) negative control of kidney. Fc; Fetal capillary, n; nucleus, IVs; Intervillous space

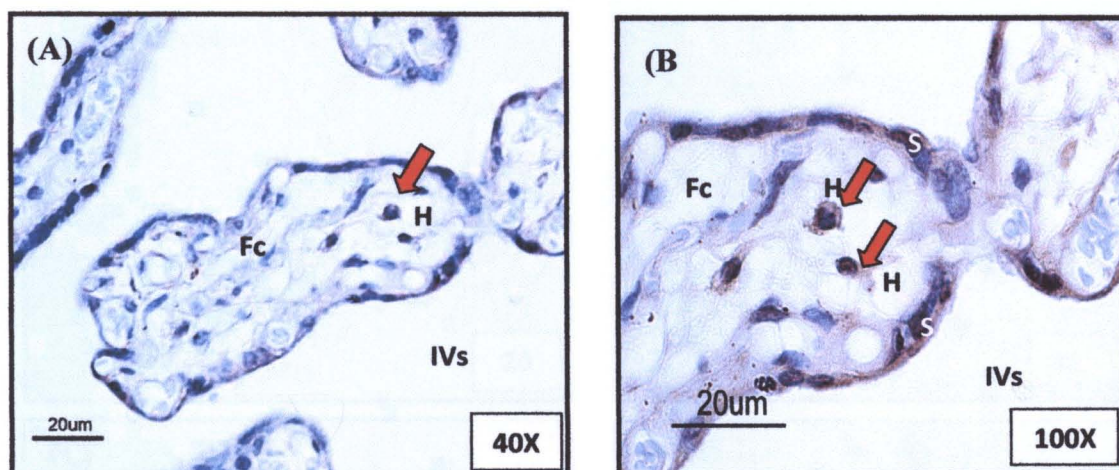


Figure 34 Localization of DMT-1 hofbuaer cell at 40X magnification and 100X (A and B, respectively; red arrow) magnifications. Syncytiotrophoblast cells, IVs; Intervillus space, Fc; Fetal capillary, H; Hofbuaer cell.

2. Maternal portion of placental tissue

In maternal portion of term human placental tissues, we observed the DMT-1 localization in decidual cells of placenta using 20X and 40X magnifications. It was found that the DMT-1 immunoreactivity was positive in placental decidual cells which was mainly in cytoplasmic area of these positive decidual cells (figure 35B and C). The negative control slide was performed by omitting the primary antibody and observed at 40X (figure 35D) magnifications.

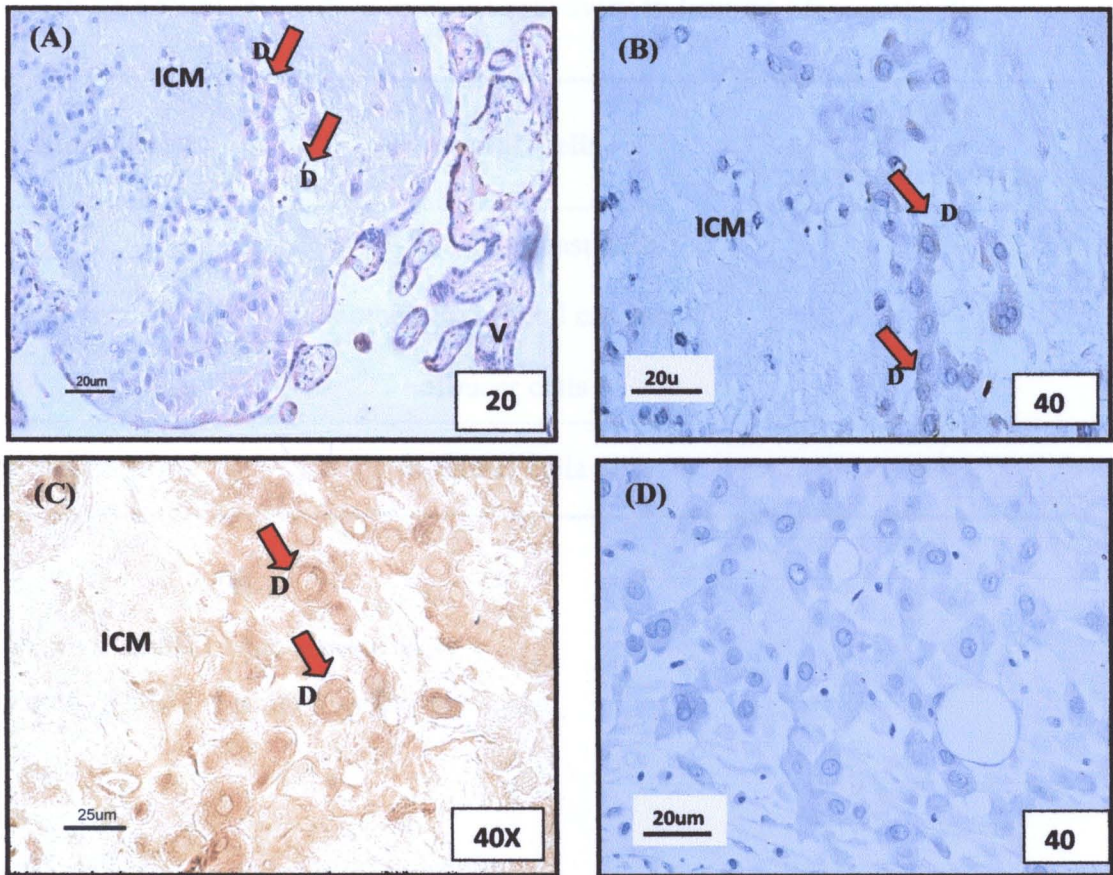


Figure 35 Localization of DMT-1 in decidual cells at 20X (A; red arrow) and 40X (B; red arrow) magnifications. (C) DMT-1 was localized only in cytoplasm of decidual cell (red arrow) and (D) negative control of placenta were also observed at 40X magnifications. D; decidual cells, ICM; Intercellular matrix, V; Villous

Table 10 The DMT-1 positive immunoreactivity in human placental cells

Placental portions	Placental Cells	DMT-1 immunoreactivity
	syncytiotrophoblast cells	+
Fetal portion	endothelium of fetal capillary	+
	hofbuaer cells	+
Maternal portion	decidual cells	+

+ ; positive DMT-1 immunoreactivity

- ; negative DMT-1 immunoreactivity

3. Localization of DMT-1 in placental barrier

A placental barrier in full term placenta, this site consists of cytoplasm of STB and endothelium of the fetal capillary as shown in figure 35A. Focusing on the placental membrane portion, the DMT-1 was predominantly localized in cytoplasm of STB and also detected along the endothelium of the fetal capillary. In order to define clearly, the expansion of placental membrane was applied and shown in figure 36B. The STB area was represented as the red dotted line in figure 36C where the DMT-1 positive immunoreactivity was obviously localized in nucleus and cytoplasm of syncytiotrophoblast cell. The fetal capillary area was represented as the yellow dotted line in figure 36C where can be seen the positive immunoreactivity of DMT-1 along the endothelium lining.

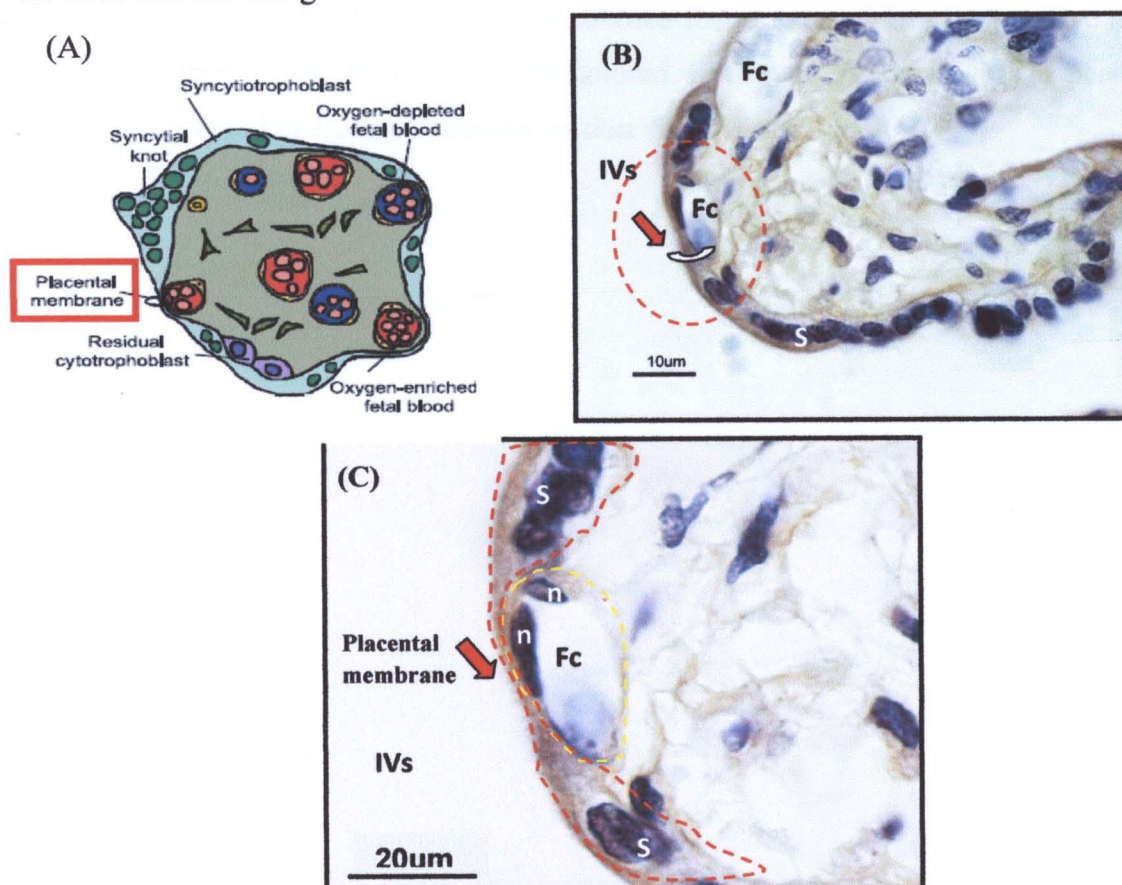


Figure 36 (A) The drawing diagraph showing placental membrane (B) DMT-1 localization in placental membrane observed under 100X (C) The expansion picture of placental membrane. S; syncytiotrophoblast cells, IVs; intervillous space, Fc; fetal capillary, n; nucleus of endothelial cell of fetal capillary.

4. Comparison of DMT-1 protein expression in STB in different areas of placenta; insertion, central and marginal areas.

After localization of DMT-1 protein in placental tissues, we also counted the number of DMT-1 positive cells in STB per total STB was shown in figure 37 to compare the DMT-1 positive immunoreactivity in STB between three areas including insertion, central and marginal areas and compared between low-Cd and high-Cd groups in each placental section. Each placental section was observed in 5 different areas (figures) at 40x magnification. The criterion using for defining STB were as followed 1.) STB defined as the peripheral cell of placental villi. 2.) Because STB is the multinucleated cell. Then, STB nucleus between 1-10 nucleuse was counted as one cell. 3.) STB (> 10 nucleuses) was classified as syncytial knot. Then, it was not counted as STB. The criterion using for counted the number of DMT-1 positive STB was STB which appeared intense brown colored. Both total STB and DMT-1 positive STB were counted in 3 complete cross section villi in each figure.

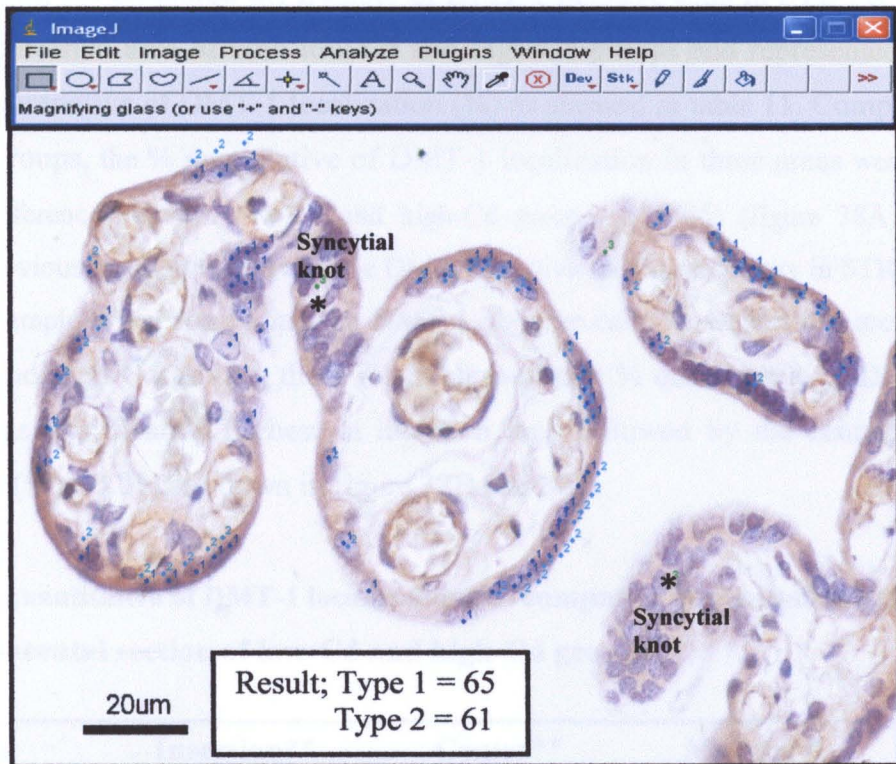


Figure 37 Counting of the number of DMT-1 positive cells in STB (type 2) per total STB (type 1) of three villi including V1, V2 and V3 by Image J software at 40X magnification. IVs; intervillous space, V; villi, V1; 1st villous, V2; 2nd villous, V3; 3rd villous



Then, we measured the number of DMT-1 positive cells in STB per total STB in each placental area of both low-Cd and high-Cd groups and represented this value as the quantitative of DMT-1 localization (%) as showed in table 11. Comparing between two groups, the % quantitative of DMT-1 localization in three areas were not significantly difference between low-Cd and high-Cd groups ($p>0.05$) (figure 38A) that related to the previous result in observing the DMT-1 positive immunoreactivity in STB cells from high micrograph. When comparing the DMT-1 positive cells between three areas of both low-Cd and high-Cd groups, these result showed that % quantitative of DMT-1 localization was significantly highest in insertion area followed by the central and marginal areas (** $p<0.01$) as shown in figure 38B and 38C.

Table 11 The quantitative of DMT-1 localization (%) compared between three areas of placental section of low-Cd and high-Cd groups

Group	Insertion**	Center**	Margin**
low-Cd group	80.96± 4.47	67.4± 7.69	49.96±6.98
high-Cd group	81.28± 3.97	71.23± 5.18	52.41± 7.38

Values represent as mean ± SEM. (** $p < 0.01$; significant between three areas, n = 6 / group)

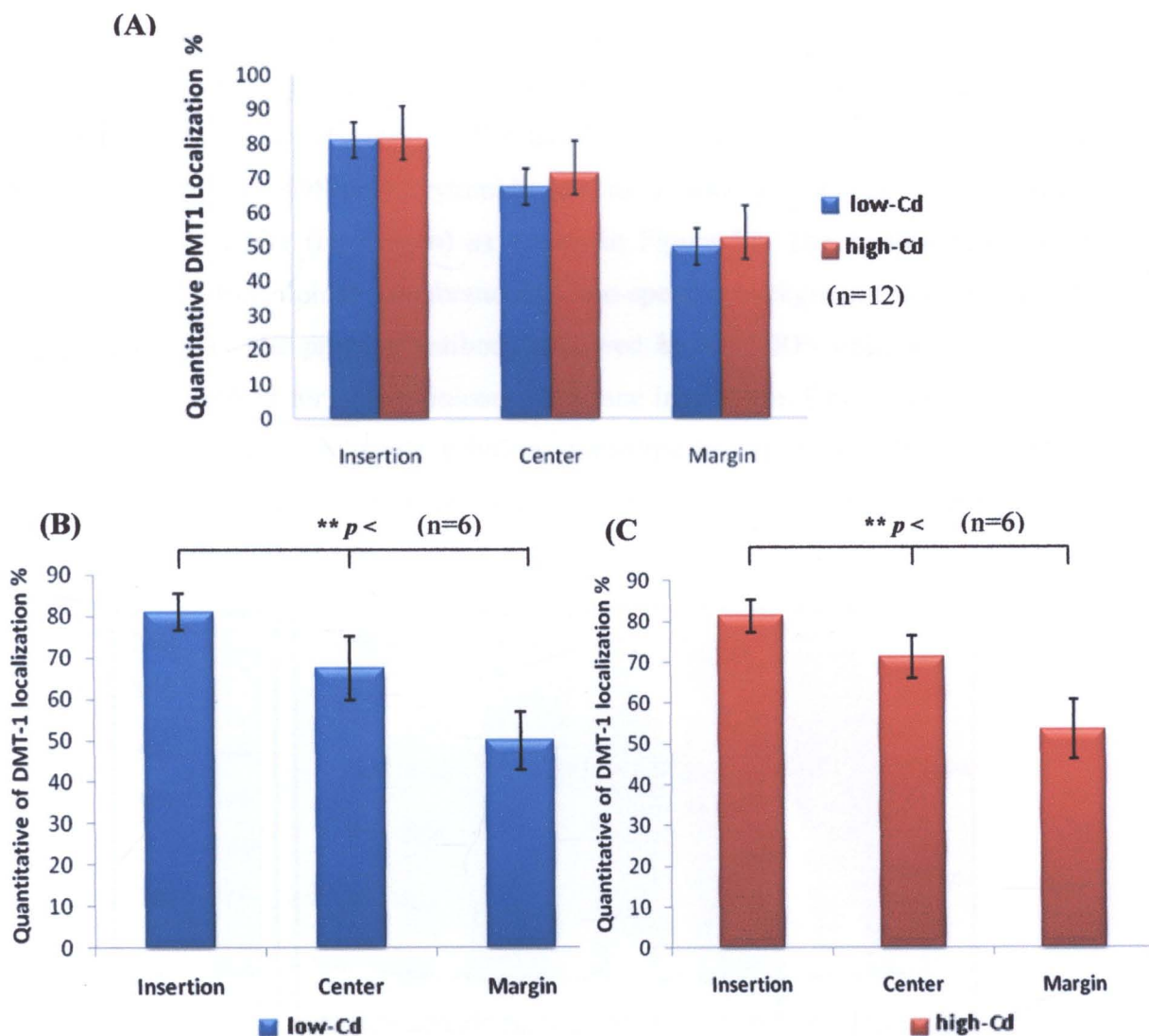


Figure 38 (A) The % quantitative of DMT-1 localization in three areas compared between low-Cd (blue bar) and high-Cd (red bar) groups (n=12), (B) The % quantitative of DMT-1 localization in three areas of low-Cd group and (C) The % quantitative of DMT-1 localization in three areas of high-Cd group

DMT-1 protein expression in placental tissues

We investigated the DMT-1 protein expression in placental tissues of high-Cd and low-Cd groups (n=6/ group) by Western blot analysis. The placental tissues were electrophoresed on SDS-polyacrylamide gel to separated placental protein bands compared with ladder (invitrogen) as shown in Figure 39. The protein bands were transferred to nitrocellulose membrane and non-specific background was blocked by using skim milk. The primary antibody followed by the HRP-conjugated secondary antibody was applied for nitrocellulose membrane incubation. Finally, this membrane was incubated in ECL substrate solution, according to expose membrane on X-ray film. The 65 Kda, DMT-1 protein bands were detected on X-ray film and β -Actin bands were defined at 43 kDa.

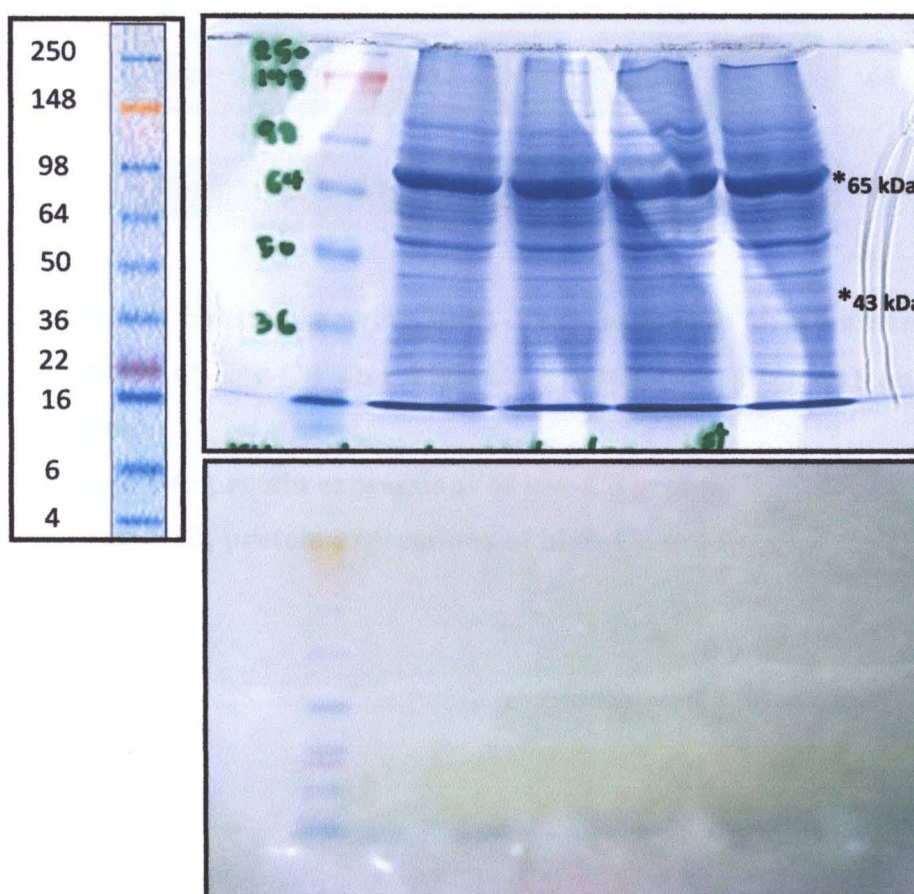


Figure 39 The photograph of placental protein bands on SDS-PAGE (right; above), transferred to membrane (right; under) and compared with SeeBlue® Plus2 Pre-Stained Standard (Left)

The intensity of DMT-1 protein expression between low-Cd and high-Cd groups was examined. The result showed that DMT-1 protein expression in high-Cd group was likely higher than in low-Cd group as shown in Figure 40. The β -Actin protein was used as the positive control protein.

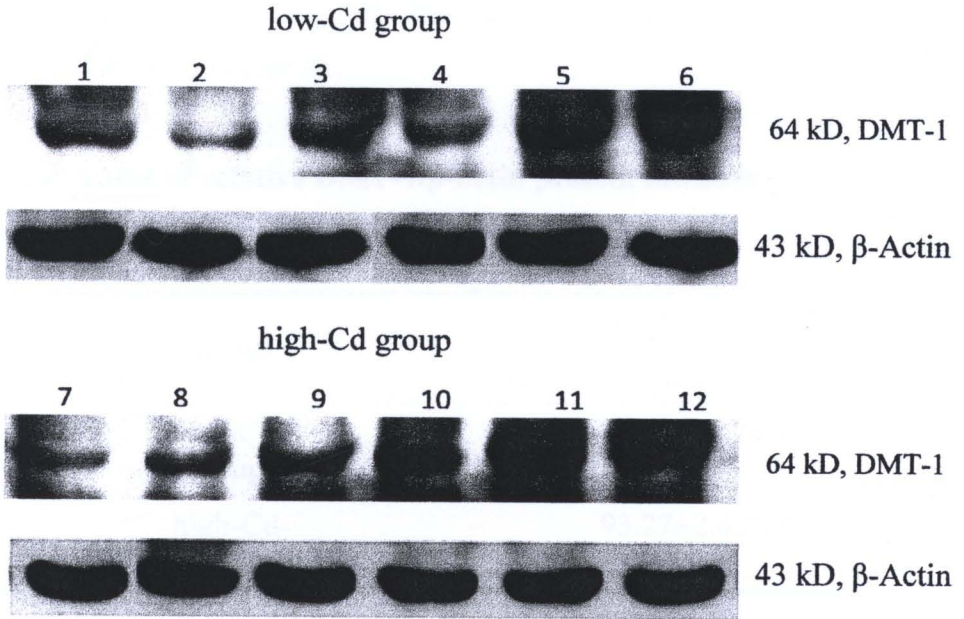


Figure 40 Western blotting showing DMT-1 expressions in term human placental tissues of low-Cd and high-Cd groups (n = 6/group) and β -Actin protein

Lane 1-6; protein expressions of low-Cd group

Lane 7-12; protein expressions of high-Cd group

We measured the intensity of both low-Cd and high-Cd groups by Scion image software. The result showed that the mean value of relative DMT-1 protein intensity in high-Cd group was $93.27 \pm 2.43\%$ and this value in low-Cd group was $78.74 \pm 2.24\%$ as shown in table 12. The statistical analysis found that the relative DMT-1 protein intensity in high-Cd group was significantly higher than in low-Cd group ($p = 0.001$) as shown in Figure 41.

Table 12 The mean value of relative DMT-1/ β -actin protein intensity

Group	DMT-1/ β -actin protein
low-Cd group	$78.74 \pm 2.24\%$ (n=6)
high-Cd group	$93.27 \pm 2.43\%^{**}$ (n=6)

Values represent as mean \pm SEM. (** $p < 0.01$, n= 6/ group)

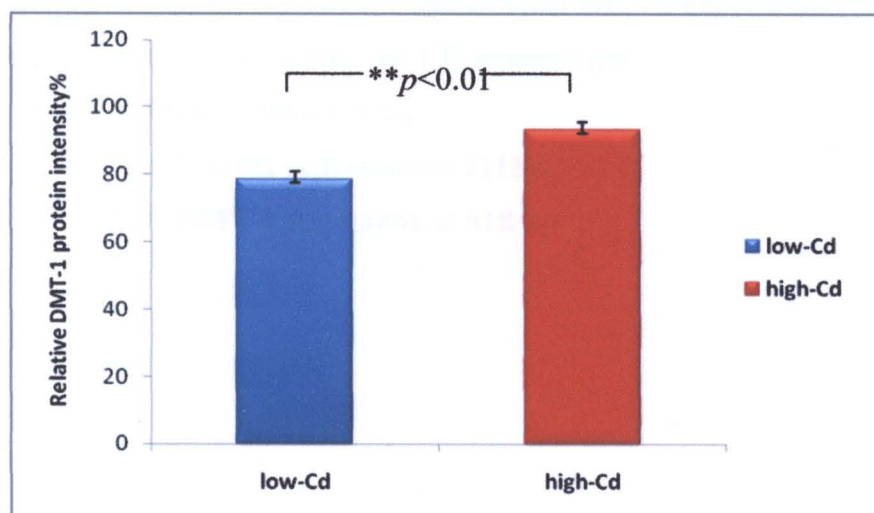


Figure 41 Quantitative analysis of DMT-1 protein in placental tissues ($p < 0.01$, n= 6/ group)**

DMT-1 mRNA expression in placental tissues

In addition, we investigated the DMT-1 gene expression in placental tissues of high-Cd and low-Cd groups by reverse transcription polymerase chain reaction (RT-PCR) method (n=6/ group). The cDNA template was amplified with specific primer of DMT-1 gene. The PCR products were electrophoresed on 1% agarose gel. The bands were detected and visualized by staining with ethidium bromide. In this study, the DMT-1 bands were detected at 518 bp. β -Actin was used as positive house keeping gene were detected at 211 bp as shown in Figure 42.



Figure 42 The photograph of DMT-1 and β -actin mRNA expressions in term human placental tissues on 1% agarose gel

Lane 1; ladder (invitrogen)

Lane 2-4; β -Actin represent at 211bp

Lane 5-7; DMT-1 represent at 518 bp

The intensity of DMT-1 mRNA expression between low-Cd and high-Cd groups was compared. The result showed that DMT-1 protein expression in high-Cd group was likely higher than that in low-Cd group as shown in Figure 43.

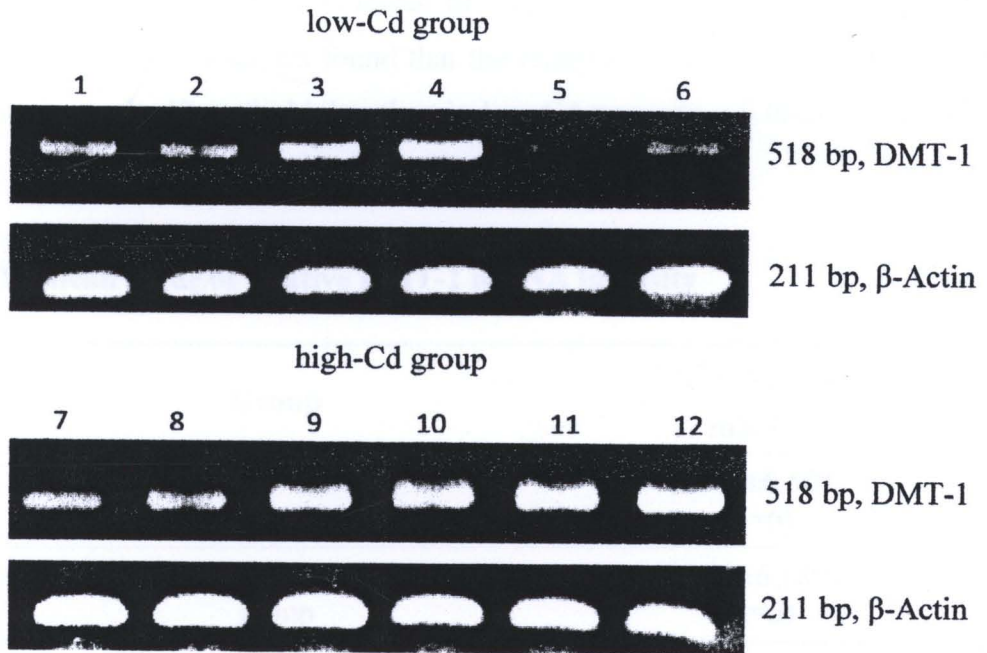


Figure 43 RT-PCR of DMT-1 mRNA expression in placental tissues of low-Cd and high-Cd groups (n = 6/group)

Lane 1-6; mRNA expressions of low-Cd group

Lane 7-12; mRNA expressions of high-Cd group

We measured the intensity of DMT-1 and β -actin expressions of both low-Cd and high-Cd groups by Scion image software. And, DMT-1 was normalized with β -actin. The result showed that the mean value of relative DMT-1 mRNA intensity in high-Cd group was $95.40 \pm 6.18\%$ whereas this value in low-Cd was $73.09 \pm 6.50\%$ (Table 13). The statistical analysis found that the relative DMT-1 mRNA intensity in high-Cd group was significantly higher than in low-Cd group ($p = 0.032$) as shown in Figure 44.

Table 13 The mean value of relative DMT-1 mRNA intensity

Group	DMT-1/ β -actin mRNA
low-Cd group	$73.09 \pm 6.50\%$ (n=6)
high-Cd group	$95.40 \pm 6.18\%^*$ (n=6)

Values represent as mean \pm SEM. ($*p < 0.05$, n= 6/ group)

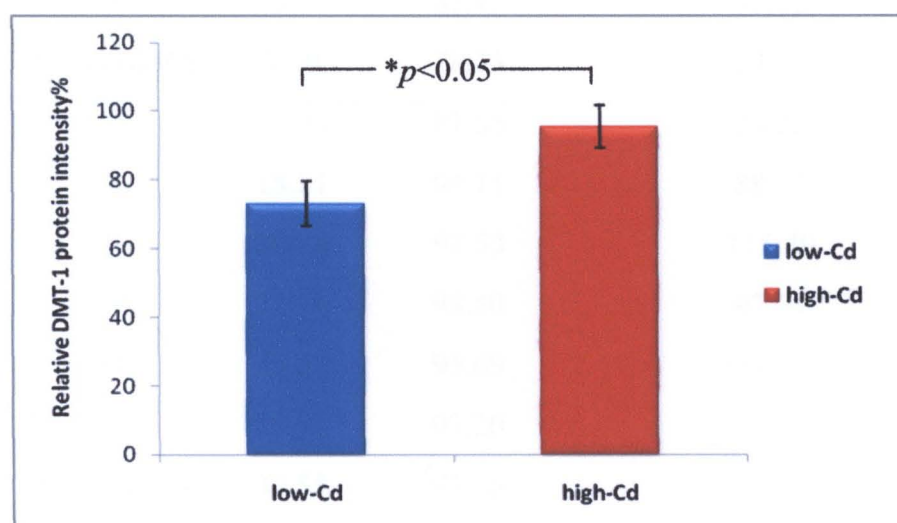


Figure 44 Quantitative analysis of DMT-1 mRNA in placental tissues ($*p < 0.05$, n= 6/ group)

We also investigated correlation between DMT-1 protein and mRNA expressions, the value of relative DMT-1 protein and mRNA intensity (%) were shown in Table 14. The correlation between DMT-1 protein and mRNA expressions in term human placentas were also investigated. The % relative values of DMT-1 protein and mRNA of both low-Cd and high-Cd groups were shown in table 14. The results showed that there was a significantly positive correlation between DMT-1 protein and mRNA expressions in placental tissues ($r = 0.847$, $**p = 0.001$) as shown in Figure 45.

Table 14 The mean value of relative DMT-1/ β -actin protein and mRNA intensity

Group	Case No.	Placental Cd ($\mu\text{g}/\text{kg}$)	Relative DMT-1/ β -actin intensity (%)	
			Protein	Gene
low-Cd	1	2.5	85.86	89.93
	2	8.5	76.43	51.14
	3	8.5	70.30	68.39
	4	8.5	77.31	60.15
	5	8.5	79.08	89.81
	6	8.5	83.43	79.12
	Mean (n=6)	7.50	78.73	73.09
high-Cd	7	50.01	81.55	70.22
	8	18.21	94.11	88.53
	9	80.78	97.53	115.79
	10	22.74	93.50	97.54
	11	33.57	95.69	100.06
	12	19.98	97.20	100.21
	Mean (n=6)	37.55	93.26	95.39



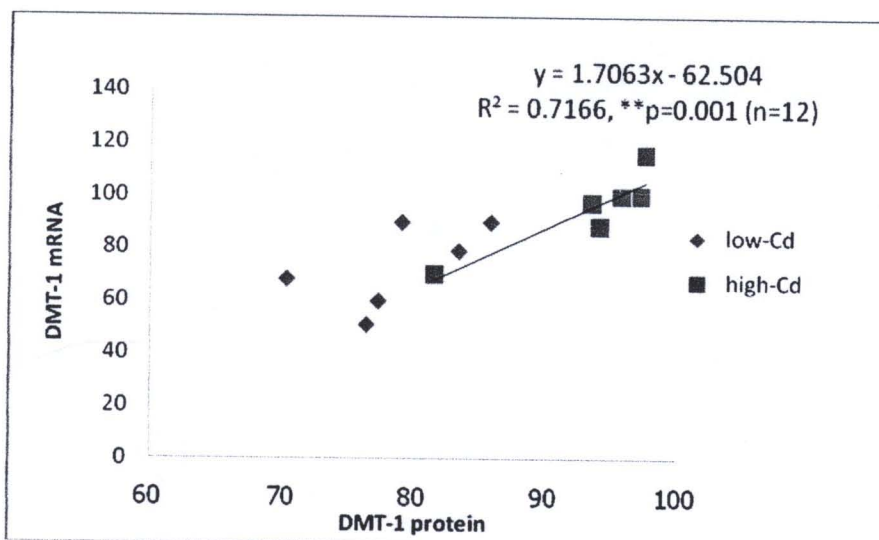


Figure 45 The correlation between DMT-1 protein and mRNA expression ($p < 0.01$)**

We also investigated correlation between placental Cd and DMT-1 expressions, all data were shown in Table 14. The correlation between placental Cd and DMT-1 protein expression was shown in Figure 46. This result showed that there trended to positive correlation between placental Cd and DMT-1 protein expression in placental tissues ($r = 0.516, p = 0.086$). In addition, the correlation between placental Cd and DMT-1 mRNA expression also trended to positive correlation in placental tissues ($r = 0.525, p = 0.079$) as shown in Figure 47.

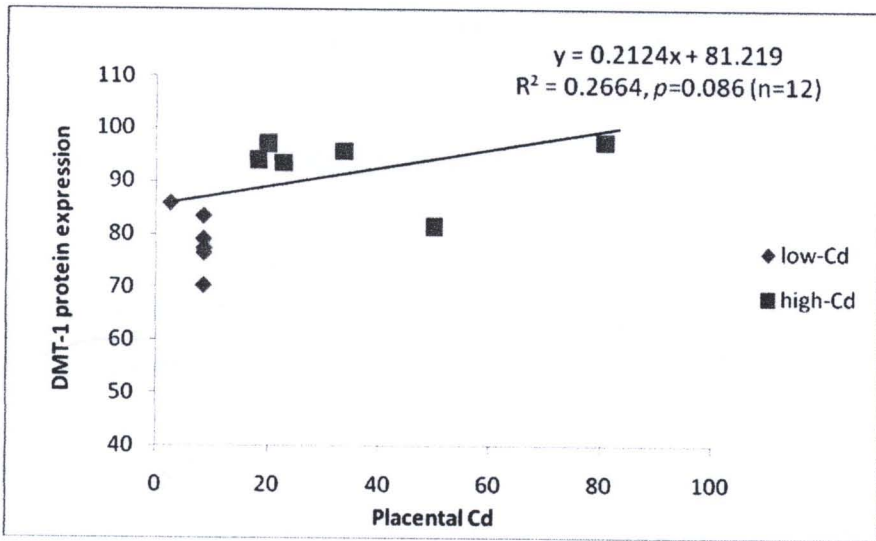


Figure 46 The correlation between placental Cd and DMT-1 protein expression

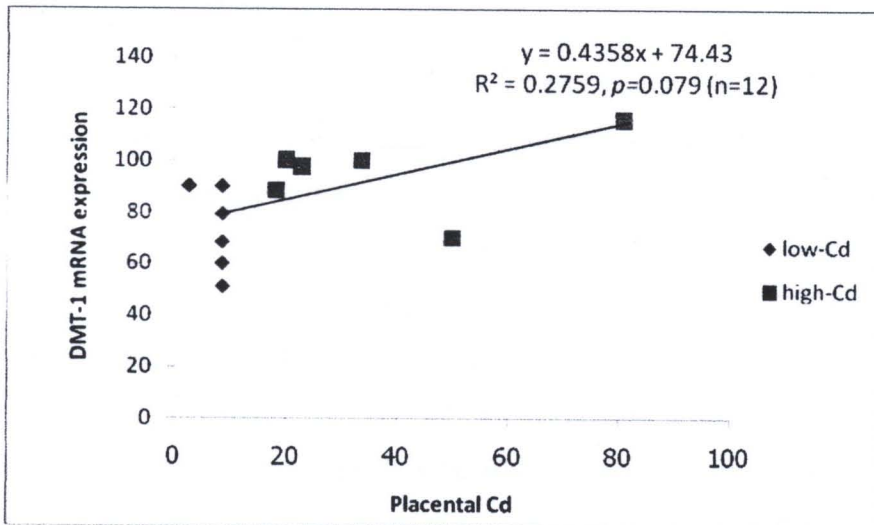


Figure 47 The correlation between placental Cd and DMT-1 mRNA expression